Volume 1 | Number 1 | Jan 2013 | Pages 1–100

PCCP

Physical Chemistry Chemical Physics
www.rsc.org/pccp

ROYAL SOCIETY OF CHEMISTRY

ROYAL SOCIETY OF CHEMISTRY

www.rsc.org/pccp

ChemComm

COMMUNICATION

Fullerene-like boron clusters stabilized by endohedrally doped iron atom: B$_n$Fe with n = 14, 16, 18 and 20

Nguyen Minh Tam,[a,b] **Hung Tan Pham,**[a] **Long Van Duong,**[a] **My Phuong Pham-Ho,**[a] **Minh Tho Nguyen**[b,*]

Stabilized fullerene and tubular forms can be produced in boron clusters B$_n$ in small sizes from n ~ 14 upon doping by transition metal atoms. B$_{14}$Fe and B$_{16}$Fe are stable tubes whereas B$_{18}$Fe and B$_{20}$Fe are stable fullerenes. Their formation and stability suggest the use of dopants to induce different growth paths leading to larger cages, fullerenes and tubes of boron.

Boron compounds exhibit extremely rich structural features. In the solid state, elemental boron is well-known to exist in the forms of amorphous, α- and β-rhombohedral allotropies, and in boron-rich compounds such as boranes and their numerous derivatives. Aggregates of the boron elements such as clusters,[1] sheets[2] and nanotubes[3-5] have been prepared or predicted, and indeed they showed many structural peculiarities.[6]

Concerning gas phase boron clusters B$_n$, a plethora of two-dimensional (2D, planar and quasi-planar) and three-dimensional (3D, tubular, cage, spherical, fullerene...) shapes were identified, suggesting several distinct growth patterns.[7-18] In relation to C$_{60}$, particular attention has been paid to the boron buckyball B$_{80}$,[19-22] and the larger fullerene derivatives such as B$_{100}$[2,23] and B$_{112}$.[24] A number of smaller all-boron fullerenes were also identified by computations including B$_{14}$, B$_{32}$, B$_{38}$, B$_{40}$, B$_{44}$, B$_{50}$ and B$_{56}$.[14,25-32] The B$_{30}$ cluster was demonstrated to have a bowl-shaped ground state structure, and the bowl B$_{30}$ constitutes an appropriate building-block whose recombination and addition could eventually lead to the generation of B$_{80}$, B$_{90}$ and B$_{92}$ buckyballs.[32] Of the smaller boron clusters, the B$_{14}$ and B$_{40}$ fullerene-like neutrals were found to be the global minima at these sizes.[14,27]

A B$_{40}$ fullerene-type is characterized by two hexagonal faces and in particular four heptagonal faces. It has a high symmetry (D_{2d}) in which the C_2 axis is going through the two hexagons. The MOs of this fullerene-like B$_{40}$ closely mimic those of the buckyball B$_{80}$.[27] Such a B$_{40}$ fullerene was recently observed by experiment using the photoelectron spectroscopy.[29]

Interest in small finite-size and stable fullerenes led to intensive search for novel building blocks for nanostructures. In this respect, the doping of a cluster has often been used to stabilize and modify the structure and properties of the resulting doped cluster. For some specific sizes, the dopant can drastically alter not only the thermochemical stability, but also electronic and magnetic properties.[33-36] Doping by metallic elements was frequently used to compensate the inherent electron deficiency of boron atoms. In the typical case of MgB$_2$, the Mg dopant injects electrons into the hexagonal B network in such a way that the electron transfer makes the Mg-doped boron semiconductors behave like a carbon graphite.[6]
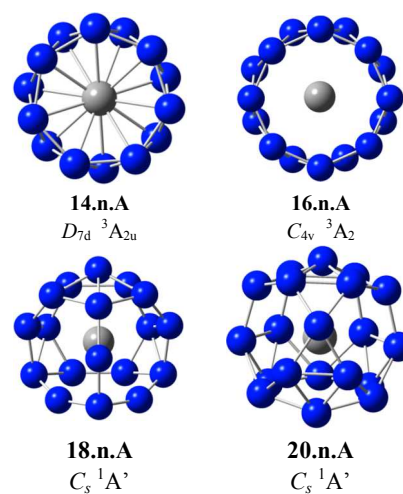

Figure 1. Shapes, point group and electronic states of the most stable isomers B$_n$Fe with n = 14, 16, 18, 20 obtained using TPSSh/6-311+G(d) computations.

Along this line, a number of small planar cyclic boron clusters doped by transition metals have been reported. These include the B$_8$M$^-$, B$_9$M$^-$ with M = Co, Fe, Ni,[37,38] or 3rd period elements.[39] In the series of B$_n$M$^-$ with n = 3-10 and M = V and Ta, these doped anionic clusters were observed experimentally,[40] but the doped clusters also exhibits different shapes ranging from 3D (boat-like, pyramid-like) to 2D molecular wheels in which the boron atom is basically multi-coordinated. There is a competition between B-B and M-B interaction in determining the most stable structures of the doped clusters. It is

clear that with such small sizes, no cage-like or fullerene-like boron structures could be formed. Endohedral doping of the buckyball B_{80} by transition metals, or organic species[41] has also been explored, but in such a large hollow medium, chemical reactions could often be occurred.

Recently, we found that small size clusters such as Si_8,[42] Si_{10},[43] Ge_{12}[44] and Si_{14}[45] can already encapsulate a metallic element such as Be, Co, Li and Mn giving quite stabilized doped clusters Si_8Be, $Si_{10}Co$, $Ge_{12}Li^+$ and $Si_{14}Mn^+$, respectively, in such a way that the resulting endohedrally doped clusters correspond to the lowest-lying isomers, and the high spin of the metallic dopant could completely be quenched. In this context, we set out to search for small size fullerene-like boron clusters that could be stabilized following endohedral doping by transition metals by using a similar strategy.

Considering the fact that B_{14} has already a stable fullerene-like geometry, and B_{20} has a double ring tube, we thus take the series of B_{14}, B_{16}, B_{18} and B_{20}, and then dope them successively with different first-row transition metals ranging from Sc to Cu. For each metallic element, we considered different charge and spin states. In the present communication, we report the promising results obtained for the iron doped boron clusters B_nFe, that reveal some novel structural and electronic features. We first search for lower-lying structures, and subsequently analyze their bonding phenomena.

Computational methods are given in the Supplementary information (ESI) file. We used density functional theory with the TPSSh and B3P86 functionals in conjunction with the 6-311+G(d) basis set for geometries, frequencies and energies. Geometries and relative energies of the lower-lying isomers are given in the Supplementary file (ESI). The shape of the lowest lying isomers of $B_{14}Fe$, $B_{16}Fe$, $B_{18}Fe$ and $B_{20}Fe$ are displayed in Figure 1. The results obtained by both functionals are similar to each other. To simplify the presentation of data, only TPSSh results are given hereafter. Let us first briefly describe the structural and energetic aspects of the doped B_nFe clusters.

i) $B_{14}Fe$ clusters. The energy ordering of the four lowest-lying isomers is displayed in the Figure S1 of the ESI. . Each of the two most stable isomers corresponds to a double ring (DR) composed of two seven-membered rings in an anti-prism form and doped by the Fe atom at the center of the cylinder. The high symmetry (D_{7d}) and high spin $^3A_{2u}$ **14-n-A** (Figure 1) turns out to be ~0.1 eV more stable than the low-spin counterpart. Interaction of the Fe atom with the fullerene-like B_{14} structure does not lead to a low-energy fullerene adduct but the resulting doped cluster has a semi-closed low spin structure (**B14.Fe.n.C**, C_{2v}, $^1A_1$, Figure S1 of Supplementary Information). The overall effect of a Fe attachment to B_{14} is the emergence of the DR as the lowest-lying structure.

ii) $B_{16}Fe$ clusters. The energy ordering of $B_{16}Fe$ clusters calculated using the TPSSh functional is shown in Figure S2 of the ESI, in which **16.n.A** (C_{4v}, $^3A_2$) structure is the most stable isomer. . The pure B_{16} cluster exhibits a symmetrical planar shape (C_{2h}, ^1A_g)[9] which is ~7 kcal/mol higher in energy (PBE/6-311+G(d) + ZPE) than the DR form composed of two eight-membered rings. As in the previous case, attachment of a Fe atom favours the doped-DR form. The triplet state **16-n-A** shown in Figure 1 is preferred over a distorted low-symmetry closed-shell state and a high symmetrical quintet state (Figure S2 of the ESI).

Figure 2 displays the partial and total densities of states (DOS) of the triplet DR **16-n-A** in which the α and β spin molecular orbitals are separately plotted. This illustrates a clear picture of its electronic shell. As expected, the frontier MOs are composed mainly from the $2p$(B) and $3d$(Fe) AOs, but with larger component of the boron AOs.

Its HOMO and LUMO however arise exclusively from the boron AOs. An orbital interaction correlation diagram (displayed in Figure S5 of the ESI) clearly points out the stabilization of the adduct due to orbital interactions.
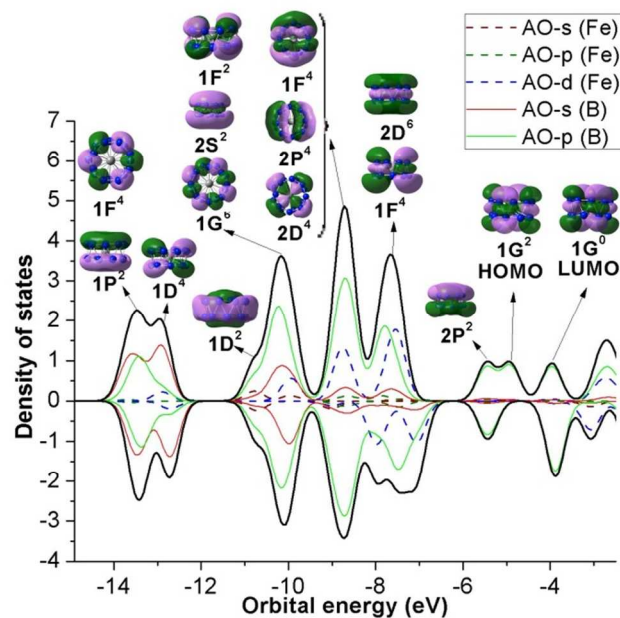

Figure 2. Total (DOS) and partial (pDOS) densities of state of $B_{16}Fe$ **16-n-A**. The shapes of MOs are obtained using TPSSh/6-311+G(d) computations.
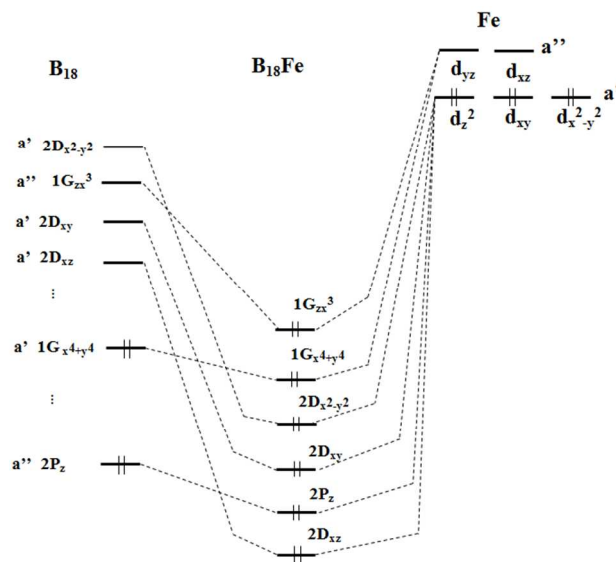

Figure 3. Orbital interaction diagram between a fullerene-like B_{18} cage and the Fe atom giving the doped cluster $B_{18}Fe$ **18.n.A**.

iii) $B_{18}Fe$ clusters. Two singlet planar structures were found to have similar energy content and thus compete for the ground state of the pure B_{18}.[9] They are a few kcal/mol lower in energy that a distorted DR formed by a

superposition of two nine-membered rings. The DR turns out to be the lowest-energy of the cation B_{18}^+.[9] The relative energy ordering of the four lower-lying $B_{18}Fe$ isomers (Figure S3 (ESI), is rather method-dependent, but the endohedrally doped cage **18-n-A** (C_s, Figure 1) remains favoured over the other isomers. The Fe dopant tends to stabilize the cage and DR forms of B_{18} more than the planar counterparts, in making the endohedrally doped **18-n-A** a lower-lying isomer. The emergence of the low-spin fullerene-like form **18-n-A** thus constitutes a remarkable effect of a Fe doping. In return, the high spin of the Fe atom is thus completely quenched following its endohedral doping. The orbital correlation diagram displayed in Figure 3 again indicates a strong stabilization of the resulting $B_{18}Fe$ MOs.

iv) $B_{20}Fe$ clusters. It is well established that lowest-lying isomer of the bare B_{20} is characterized by a DR shape,[9,10] even though the energy difference between both corresponding DR and planar counterparts is relatively small, being ~5-8 kcal/mol depending on the method employed. The doped DR **20-n-B** (Figure S4 of the ESI) has a distorted shape with an asymmetrical position of the dopant within the cylinder. This is presumably due to the fact that the space inside the B_{20} DR is too large, and thereby the B-Fe distances too long, to accommodate a symmetrical Fe atom at the center. Overall, similar to the $B_{18}Fe$ **18-n-A** structure, the emergence of an endohedrally doped fullerene-type **20-n-A** (Figure 1) having a closed-shell electronic state represents an important effect of the Fe doping. The total (DOS) and partial (pDOS) densities of states illustrated in Figure S6 (ESI) clearly point out the overlap between d orbitals of Fe and both s and p orbitals of B atoms.
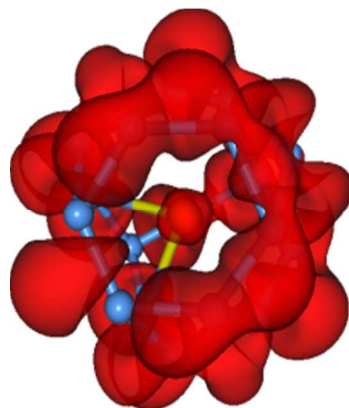
$B_{18}Fe$ 18-n-A

Figure 4. The ELF iso-surface at bifurcation value of 0.85 of the doped $B_{18}Fe$ cluster. The wave functions were obtained using the TPSSh/6-311+G(d) computations.

The electron localization function (ELF) plot of $B_{18}Fe$ displayed in Figure 4 show high ELF value of 0.85 indicating strong interaction between skeletal B_{18} bonds and the Fe dopant. No localization domains can be found between the Fe atom and B_{18} counterparts, suggesting a certain ionic character of the Fe-B bonds The NBO charge of Fe atom in $B_{18}Fe$ is about -1.0 electron in the singlet fullerene. Thus B_{18} cage actually transfers electrons to the Fe atom, and $B_{18}Fe$ cage can be seen as involving of anion Fe^- and cation B_{18}^+

fullerene. Electrostatic interaction also contributes to its thermodynamic stability. Such a situation is not uncommon. In the Mn-doped silicon fullerene $Si_{14}Mn^+$, a charge transfer is also found to take place from the Si_{14} moiety to the dopant.[45]

In summary, the most interesting result of our extensive searches on the M-doped B_nM clusters is the finding that strong effects of the Fe dopant in substantially stabilizing the double ring shape already from the size of 14 (**14-n-A**) and 16 (**16-n-A**), and the fullerene-like shape from the size of 18 (**18-n-A**) and 20 (**20-n-A**). Overall, stabilized fullerene and tubular adducts can be formed in boron clusters B_n in the smaller size range, in which the high spin of the dopant atom is partially quenched already from n ~14, and completely quenched at the sizes of 18 and 20. Their formation foreshadows different growth paths leading to larger boron cages, tubes and fullerenes.

References and Note
[a] Institute for Computational Science and Technology (ICST), Ho Chi Minh City, Vietnam.
[b] Department of Chemistry, University of Leuven, Leuven, Belgium. E-mail: minh.nguyen@chem.kuleuven.be.

1 L. Hanley and S. L. Anderson, *J. Phys. Chem*. 1987, **91**, 5161.
2 C. Ozdogan, S. Mukhopadhyay, W. Hayami, Z. B. Guvenc, R. Pandey and I. Boustani, *J. Phys. Chem. C* 2010, **114,** 4362.
3 G. Ciofani, V. Raffa, A. Menciassi and A. Cuschieri, *Nano Today*, 2009, **4**, 8.
4 A. K. Singh, A. Sadrzdeh and B. I. Yakobson, *Nano Lett*. 2008, **8,** 1314
5 I. Boustani, A. Quandt, E. Hernandez and A. Rubio, *J. Chem. Phys*. 1999, **110**, 3176.
6 H. Tang and S. Ismail-Beigi, *Phys. Rev. Lett*. 2007, **99**, 115501.
7 S. Chacko, D. G. Kanhere and I. Boustani, *Phys. Rev. B* 2003, **68** 035414.
8 H. J. Zhai, B. Kiran, J. Li and L. S. Wang, *Nature Mat*. 2003, **2**, 827.
9 T. B. Tai, M. N. Tam and M. T. Nguyen, *Chem. Phys. Lett*. 2012, **530**, 71.
10 B. Kiran, S. Bulusu, H. J. Zhai, S. Yoo, X. C. Zeng and L. S. Wang, *Proc. Nat. Acad. Sci. USA* **2005**, 102, 961..
11 W. Huang, A. P. Sergeeva, H. J. Zhai, B. B. Averkiev, L. S. Wang and A. I. Boldyrev, *Nature Chem*. 2010, **2**, 202.
12 H. T. Pham, L. V. Duong, B. Q. Pham and M. T. Nguyen, *Chem. Phys. Lett*. 2013, **577**, 32.
13 L. Jian, Y. Wang, L. Zhu and Y. Ma, *Nanoscale*, 2014
14 L. Cheng, *J. Chem. Phys*., 2012, **136**, 104301.
15 E. Oger, N. R. M. Crawford, R. Kelting, P. Weis, M. M. Kappes and R Ahlrichs, *Angew. Chem. Int. Ed*. 2007, **46**, 8503.
16 T. B. Tai, N. M. Tam and M. T. Nguyen, *Theor. Chem. Acc.*, 2012, **131**, 1241.
17 Z. A. Pizza, H. Hu, W. Li, Y. Zhao, J. Li and L. S. Wang, *Nature Com*., 2014, **5**, 3113.
18 N. G. Szwacki, A. Sadrzadeh and B. I. Yakobson, *Phys. Rev. Lett.*, 2007, **98**, 166804.
19 J. T. Muya, E. Lijnen, M. T. Nguyen and A. Ceulemans, *J. Phys. Chem. A,* 2011, **155**, 2268.
20 J. T. Muya, H. Ramanantoanina, C. Daul, M. T. Nguyen, G. Gopakumar and A. Ceulemans, *Phys. Chem. Chem. Phys.*, 2013, **15**, 2829.
21 D. E. Bean, J. T. Muya, P. W. Fowler, M. T. Nguyen and A. Ceulemans, *Phys. Chem. Chem. Phys.* 2011, **13**, 20855.

22 H. He, R. Pandey, I. Boustani and S. P. Karna, *J. Phys. Chem. C*, 2010, **114** , 4149.

23 J. T. Muya, G. Gopakumar, M. T. Nguyen and A. Ceulemans, *Phys. Chem. Chem. Phys.*, 2011, **13,** 7524.

24 L. Wang, J. Zhao, F. Li and Z. Chen, *Chem. Phys. Lett.*, 2010, **501**, 16.

25 H. Lu and S. Li, *J. Chem. Phys.,* 2013, **139**, 224307.

26 S. Botti, A. Castro, N. N. Lathiotakis, X. Andrade and M. A. L. Marques, *Phys. Chem. Chem. Phys.,* 2009, **11**, 4523.

27 H. T. Pham, L. V. Duong, N. M. Tam, M. P. Pham-Ho and M. T. Nguyen, *Chem. Phys. Lett.*, 2014, **608**, 295.

28 X. Sheng, Q. Yan, Q. Zheng and G. Su. *Phys. Chem. Chem. Phys.*, 2009, **11**, 9696.

29 H. J. Zhai, Y. F. Zhao, W. L. Li, Q. Chen, H. Bai, H. S. Hu, Z. A. Piazza, W. J. Tian, H. G. Lu, Y. B. Wu, Y. W. Mu, G. F. Wei, Z. P. Liu, J. Li, S. D. Li and L. S. Wang, *Nature Chem.* 2014, **6**, 727.

30 K. D. Quarles, C. B. Kah, R. N. Gunasinghe, R. N. Musin and X. Wang, *J. Chem. Theor. Comput.,* 2011, **7**, 2017.

31 W. Hayami and S. Otani, *J. Phys. Chem. A*, 2011, **115**, 8204.

32 T. B. Tai, L. V. Duong, H. T. Pham, D. T. T. Mai and M. T. Nguyen, *Chem. Commun*, 2014, **50,** 1558.

33 S. De, A.Willand, M. Amsler and P. Pochet, L. Genovese, S. Goedecker*, Phys. Rev. Lett.*, 2011, **106**, 225502.

34 P. Boulanger, M. Morinere, L. Genovese and P. Pochet*, J. Chem. Phys.*, 2013, **138**, 184302.

35 E. Janssens, H. Tanaka, S. Neukermans, R. E. Silverans and P. Lievens, *Phys. Rev. Lett.*, 2004, **90**, 033401.

36 C. Buzea and T. Yamashiat, *Supercond. Sci. Technol.,*2001, **14**, R115.

37 K. Ito, Z. Pu, Q. Li and P. v. R. Scheyer, *Inorg. Chem.,*2008, **47**, 10906.

38 Y. Liao, C. L. Cruz, P. v. R. Schleyer and Z. Chen, *Phys. Chem. Chem. Phys.*, 2012, **14**, 14898.

39 W. Li, A. S. Ivanov, J. Federic, C. Romanescu, I. Cernusak, A. I. Boldyrev and L. S. Wang, *J. Chem. Phys.*, 2013, **139**, 104312.

40 W. Li, C. Romanescu, Z. A. Piazza and L. S. Wang, *Phys. Chem.Chem. Phys.*, 2012, **14**, 13663.

41 J. T. Muya, E. Lijnen, M. T. Nguyen and A. Ceulemans, *J. Phys. Chem. A*, 2011, **115**, 2268.

42 V. T. Ngan and M. T. Nguyen, *J. Phys. Chem. A*, 2010, **114**, 7609.

43 Y. Li, N. M. Tam, P. Claes, A. P. Woodham, J. T. Lyon, V. T. Ngan, M. T. Nguyen, P. Lievens, A. Fielicke and E. Janssens, *J. Phys. Chem. A*, 2014, **118** (as soon as publishable)

44 T. B. Tai and M. T. Nguyen, *Chem. Phys. Lett*., 2010, **492**, 290.

45 V. T. Ngan, K. Pierloot and M. T. Nguyen, *Phys. Chem. Chem. Phys*., 2013, **15**, 5493.